Numerical Simulations of Ultrafast Charge Separation Dynamics from Second Excited State of Directly Linked Zinc−Porphyrin−Imide Dyads and Ensuing Hot Charge Recombination into the First Excited State

Vladimir N. Ionkin and Anatoly I. Ivanov*

Volgograd State University, University Avenue 100, Volgograd 400062, Russia

Received: July 25, 2008; Revised Manuscript Received: September 19, 2008

A model of the intramolecular charge separation from the second singlet excited-state of directly linked Zn−porphyrin−imide dyads and following charge recombination into the first singlet excited-state has been constructed and investigated. The model incorporates three electronic states (the first and the second singlet excited and charge separated states) as well as their vibrational sublevels. Dynamics of the transitions between these states are described in the framework of the stochastic point-transition approach. The relaxation of the intramolecular high frequency vibrational mode is supposed to occur as a single-quantum transition between nearest states with a time constant depending on the number of the vibrational state. The medium relaxation is characterized by two timescales. A good fitting to experimentally observed population dynamics of both the first and the second singlet excited states has been obtained. The calculations show the charge recombination into the first excited-state to proceed in a hot stage in parallel with the relaxation of both the medium and the intramolecular high-frequency vibrational mode.

I. Introduction

Over a few past decades, there have been a large number of investigations on the photoinduced charge transfer (CT) in solutions. In the vast majority of cases the charge separation (CS) from the first singlet excited state, S_1, was explored. The photoinduced processes starting with CS may be followed by the charge recombination (CR) into the ground state, S_0. The dynamics of CS and CR are expected to be very sensitive to the value of the CR free energy ΔG_{CR}.[1,2] This sensitivity can be explained in terms of the wave packets. Evidently the CS may be visualized as an appearance of a well-localized wave packet in the vicinity of the crossing point of the terms U_{S1} and U_{CS} (see Figure 1a). The created wave packet starts to move to the bottom of the U_{CS} well. This motion reflects the relaxation of the nuclear subsystem. In the case of large CR driving force, $-\Delta G_{CR} > E_r$, where E_r is the total reorganization energy, the CR proceeds in thermal regime upon completion of the relaxation. As a result, CS and CR are well separated in time and CR rate can be rather slow. In the opposite case of small CR driving force, $-\Delta G_{CR} < E_r$, the CR can mainly proceed at hot stage during wave packet motion to the well bottom (see Figure 1b).[1,3−8] In such a regime the CS and CR are not separable due to their considerable overlapping in time. In consequence of large energy gap between S_1 and the ground state S_0, the CR to the ground-state usually proceeds in the inverted region, $-\Delta G_{CR} > E_r$. There are only a few exceptions. The donor−acceptor pair consisting of perylene and tetracyanoethylene is the most known example.[2,9,10] However, most likely the CS in this pair leads to population of excited states of the radical ions so that the CR can not be interpreted in the framework of three level model presented in Figure 1, parts a and b.[9] It should be pointed out that considering here only ultrafast CR, we may neglect the singlet−triplet conversion of the radical-ion pairs and ensuing CR to the triplet excited-state of either the donor or the acceptor.

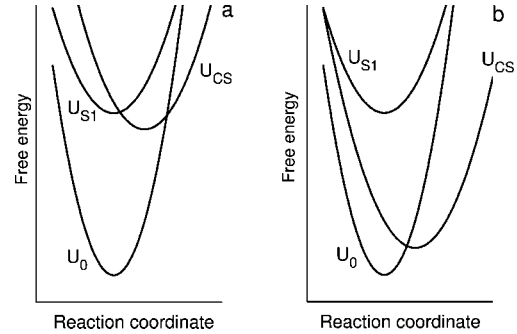

Figure 1. Schematic illustration of the difference in CS and CR for highly (panel a) and weakly (panel b) exergonic CR using the free energy curves of the ground, excited, and CS states.

A completely different type of situation occurs in CS from the second excited-state due to relatively small energy gap between the second and the first singlet excited states. In this case the CR into the first excited-state proceeds in the Marcus normal regime, and its free energy can even be positive. What this means is the dynamics and mechanism of photochemical processes started from the second excited-state are expected to differ dramatically from that started from the first excited state. Although, the elucidation of the fundamental mechanism of ultrafast CS reaction from S_2 state is very important for the photochemistry of higher excited states in condensed phase, there are very limited data on the dynamics of such reactions. Namely, the higher excited states are indeed very difficult to detect in the condensed phase because most of them are very short-lived. As a result the internal conversion is the main channel of their primary transformation. Nevertheless, there are a few examples in which the dynamics of CS from the S_2 state and ensuing CR have been investigated with high time resolution.[11−15] What is especially important, both inter- and

* To whom correspondence should be addressed. E-mail: physic@vlink.ru.

10.1021/jp806589m CCC: $40.75
Published on Web 12/08/2008

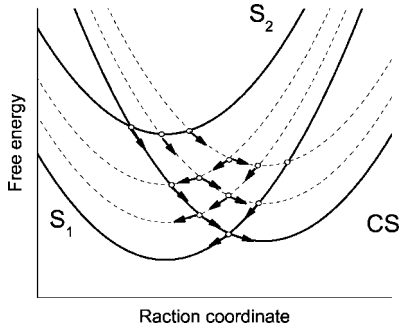

Figure 2. Schematic representation of free energy curves for CS from the second excited-state and following CR into the first singlet excited state. The dashed lines are the vibrational sublevels of CS and S_1 electronic states. The arrows stand for the directions of both the electronic transitions and the medium relaxation. The transitions between vibrational sublevels of the high-frequency mode involved in the model are not shown.

intramolecular CS from the second excited-state for the derivatives of porphyrine, one of the most significant biological molecules, can be explored.[11,15]

Detailed investigations of the CS from the second excited-state and CR to the first excited-state in a series of supramolecular systems where the Zn−porphyrine derivatives is directly linked to an electron acceptor (a series of imide compounds) were reported in refs 11−14. In what follows we use the abbreviations for these supramolecular systems suggested in refs 11−14. The dynamics of CS and CR have the following most important features. First, the rates of S_2 fluorescence decay are only slightly larger than the S_1 fluorescence rise.[14] These experimental results strongly suggest that the CS from S_2 state is followed by the S_1 state formation by CR in the curse of both the media and intramolecular vibrational relaxation.[14] The hot CR manifests itself most profoundly in the supramolecular systems with positive free energy of CR into the first excited state (the S_1 state locates above CS state). In such molecules an ultrafast rise follows by its slower decay. Apparently, such an ultrafast rise should be interpreted in terms of hot CR. Second, the internal conversion $S_2 \rightarrow S_1$ is rather slow so that the product $k_{CS}\tau_f$, where k_{CS} is the CS rate constant and τ_f is the S_2 fluorescence lifetime, is larger than 0.9 for all molecules explored except for ZP−NI for which it is about 0.7.[14] To put it differently, almost all molecules excited to S_2 undergo ultrafast CS except for only a few percent of them undergoing internal conversion. This fact allows to accept, as the first approximation, a model ignoring totally the internal conversion $S_2 \rightarrow S_1$.

The aim of this paper is an elucidation of a detailed microscopic mechanism of ultrafast intramolecular CS from the second excited state, S_2, followed by ultrafast CR into the first excited state, S_1. The model involving fast relaxation of intramolecular high frequency vibrations and explicit description of the medium relaxation is shown to constitute a quantitative description of CS and CR dynamics in series of Zn−porphyrin−imide dyads.

II. The Model of Ultrafast Charge Transfer from Second Excited State

The description of electronic transitions starting from the second singlet excited-state should account for a possibility of hot CR into the first singlet excited state. So that a minimal model should include at least three electronic states: the first and the second singlet excited states, $|S_1\rangle$, $|S_2\rangle$, correspondingly, and charge separated state, $|CS\rangle$. Energetically allowed transitions to the excited triplet and the ground states, $|S_0\rangle$, can be omitted due to their long time scale. Indeed, a few nanoseconds are required for the ground-state population recovery, while the CS from S_2 excited-state and ensuing CR proceed within a few picoseconds.

To describe real solvents with several relaxation timescales[16−19] a number of reaction coordinates are required. These reaction coordinates correspond to different relaxation modes reflecting distinct types of motions of the solvent molecules. Dynamic characteristics of the motion along the reaction coordinates can be determined from the solvent relaxation function, $X(t)$. In the framework of the Markovian approximation for solvent modes, the solvent relaxation function may be written as a sum of exponentials

$$X(t) = \sum_{i=1}^{N} x_i e^{-t/\tau_i} \tag{2.1}$$

where $x_i = E_{ri}/E_{rm}$, τ_i, and E_{ri} are the weight, the relaxation time constant, and the reorganization energy of the ith medium mode, respectively, $E_{rm} = \sum E_{ri}$, and N is the number of the solvent modes. Equation 2.1 suggests that the solvent relaxation function should appear to decay exponentially, and that means diffusional motion along each solvent mode, while an initial part of relaxation is not diffusive but rather inertial.[16−19] A possibility of approximation of the initial relaxation by exponential function and how this approximation influences on the charge transfer dynamics are discussed in ref 20.

The diabatic free energy surfaces for the electronic states in terms of the coordinates Q_i may be written as follows

$$U_{S2} = \sum \frac{Q_i^2}{4E_{ri}} \tag{2.2}$$

$$U_{CS}^{(n)} = \sum \frac{(Q_i - 2E_{ri})^2}{4E_{ri}} + n\hbar\Omega + \Delta G_{CS} \tag{2.3}$$

$$U_{S1}^{(m)} = \sum \frac{Q_i^2}{4E_{ri}} + m\hbar\Omega + \Delta G_{12} \tag{2.4}$$

where Ω and n,m (n,m = 0, 1, 2,...) are the frequency and quantum numbers of the effective intramolecular quantum mode, correspondingly, ΔG_{CS} is the CS free energy from the second excited state S_2, ΔG_{12} is the free energy gap between the first and the second excited states.

The processes considered in this paper include the CS chiefly proceeding in thermal regime and CR occurring at highly nonequilibrium conditions. This leads to the problem of nonequilibrium electronic transitions that has been already addressed from different points of view.[1,3,21−33] Since the charge transfer dynamics should be simulated in the case of highly efficient hot recombination, the perturbation theory in electronic coupling is not applicable. To get an appropriate description, we use the stochastic point-transition approach[34] generalized to a multilevel system.[6,20]

The temporal evolution of the system is described by a set of equations for the probability distribution functions for the second excited state $\rho_{S2}(\mathbf{Q},t)$, for the mth sublevel of the first excited state $\rho_{S1}^{(m)}(\mathbf{Q},t)$ and for the nth sublevel of the charge-separated state $\rho_{CS}^{(n)}(\mathbf{Q},t)$

$$\frac{\partial \rho_{S2}}{\partial t} = \hat{L}_S \rho_{S2} - \sum_n k_n^{CS} \rho_{S2} \quad (2.5)$$

$$\frac{\partial \rho_{CS}^{(n)}}{\partial t} = \hat{L}_{CS} \rho_{CS}^{(n)} + k_n^{CS} \rho_{S2} - \sum_m k_{nm}^{CR} (\rho_{CS}^{(n)} - \rho_{S1}^{(m)}) + \frac{1}{T_v^{(n+1)}} \rho_{CS}^{(n+1)} - \frac{1}{T_v^{(n)}} \rho_{CS}^{(n)} \quad (2.6)$$

$$\frac{\partial \rho_{S1}^{(m)}}{\partial t} = \hat{L}_S \rho_{S1}^{(m)} - \sum_n k_{nm}^{CR} (\rho_{S1}^{(m)} - \rho_{CS}^{(n)}) + \frac{1}{T_v^{(m+1)}} \rho_{S1}^{(m+1)} - \frac{1}{T_v^{(m)}} \rho_{S1}^{(m)} \quad (2.7)$$

where $\mathbf{Q}$ stands for the vector with components $Q_1, Q_2, \ldots, Q_N$, $\hat{L}_{CS}$ and $\hat{L}_S$ are the Smoluchowski operators describing diffusion on the U_{CS} and on the U_{S2} and U_{S1} potentials

$$\hat{L}_S = \sum_{i=1}^{N} \frac{1}{\tau_i} \left[1 + Q_i \frac{\partial}{\partial Q_i} + \langle Q_i^2 \rangle \frac{\partial^2}{\partial Q_i^2} \right] \quad (2.8)$$

$$\hat{L}_{CS} = \sum_{i=1}^{N} \frac{1}{\tau_i} \left[1 + (Q_i - 2E_{ri}) \frac{\partial}{\partial Q_i} + \langle Q_i^2 \rangle \frac{\partial^2}{\partial Q_i^2} \right] \quad (2.9)$$

with $\langle Q_i^2 \rangle = 2E_{ri}k_BT$ being the dispersion of the equilibrium distribution along the ith coordinate. Here k_B is the Boltzmann constant and T is the temperature.

The coupling parameters $k_n^{CS} = k_n^{CS}(\mathbf{Q})$ and $k_{nm}^{CR} = k_{nm}^{CR}(\mathbf{Q})$ are the Zusman rates of charge transfer between U_{S2} and $U_{CS}^{(n)}$ and between $U_{CS}^{(n)}$ and $U_{S1}^{(m)}$, respectively. In the case of a charge separation reaction, the Zusman rates take the form

$$k_n^{CS} = \frac{2\pi V_n^2}{\hbar} \delta(U_{S2} - U_{CS}^{(n)}), \quad V_n^2 = V_{CS}^2 F_n,$$

$$F_n = \frac{(S^{(CS)})^n \exp\{-S^{(CS)}\}}{n!}, \quad S^{(CS)} = \frac{E_{rv}^{(CS)}}{\hbar\Omega}$$

For the charge transfer between CS and S_1 states the Zusman rates take another more common form

$$k_{nm}^{CR} = \frac{2\pi V_{nm}^2}{\hbar} \delta(U_{CS}^{(n)} - U_{S1}^{(m)}), \quad V_{nm}^2 = V_{CR}^2 F_{nm},$$

$$F_{nm} = \exp\{-S^{(CR)}\} n!\, m! \left[\sum_{r=0}^{\min(n,m)} \frac{(-1)^{n-r} \left(\sqrt{S^{(CR)}}\right)^{n+m-2r}}{r!\,(n-r)!\,(m-r)!} \right],$$

$$S^{(CR)} = \frac{E_{rv}^{(CR)}}{\hbar\Omega},$$

where F_{nm}, $S^{(CR)}$, and E_{rv} are the Franck−Condon, the Huang−Rhys factors, and the reorganization energy of the effective high-frequency vibrational mode, respectively. The indexes (CS) and (CR) stand for the parameters relating to the CS or CR processes, correspondingly.

We adopt here a single-quantum mechanism of high-frequency mode relaxation and the transitions $n \rightarrow n - 1$ to proceed with the rate constant $1/\tau_v^{(n)}$. Naturally, the ground vibrational state is stable. The dependence of the relaxation time on n is supposed to be $\tau_v^{(n)} = \tau_v^{(1)}/n$.[35]

It should be noted that eq 2.5 ignores completely the reversibility of the reaction of CS from the second excited state, S_2. This approximation is suitable for the systems considered because the CS proceeds in either nearly activationless or inverted regimes where the reversibility has insignificant effect.[7]

TABLE 1: Parameters of CS and CR of ZP−I Series, in eV

	ΔG_{CS}[a]	ΔG_{CR}[a]	ΔG_{CS}	ΔG_{CR}	$V_{CS} = V_{CR}$
ZP−NI	−1.42	+0.74	−1.37	+0.69	0.023
ZP−PI	−1.15	+0.47	−1.09	+0.41	0.030
ZP−Cl_4PH	−0.87	+0.19	−0.96	+0.28	0.035
ZP−Cl_2PH	−0.68	+0.00	−0.74	+0.06	0.033
ZP−ClPH	−0.63	−0.05	−0.73	+0.05	0.032
ZP−PH	−0.57	−0.11	−0.75	+0.07	0.026
ZP−MePH	−0.56	−0.12	−0.77	+0.09	0.022

[a] The data are taken from ref 14.

We assume that the system initially in the ground-state with a thermal distribution of the nuclear coordinates, is transferred to the second excited state $|S_0\rangle \rightarrow |S_2\rangle$ by a short pump pulse. Since the excitation does not include a considerable charge redistribution, the equilibrium state of the polar medium immediately after excitation may be accepted as a good approximation. The excitation wavelength used in the experiments is near to the red edge of the absorption band of the transition $|S_0\rangle \rightarrow |S_2\rangle$ therefore the intramolecular high frequency modes are supposed to be in their ground state. It allows one to specify the initial conditions in the form

$$\rho_{S2}(\mathbf{Q}, t=0) = \prod_i \frac{1}{\sqrt{2\pi\langle Q_i^2 \rangle}} \exp\left[-\frac{Q_i^2}{2\langle Q_i^2 \rangle} \right] \quad (2.10)$$

$$\rho_{CS}^{(n)}(\mathbf{Q}, t=0) = 0, \quad \rho_{S1}^{(m)}(\mathbf{Q}, t=0) = 0 \quad (2.11)$$

The set of eqs 2.5−2.7 with the initial conditions eqs 2.10−2.11 was solved numerically using the Brownian simulation method.[2,20,36]

We pause here to schematically describe the physical processes incorporating into the model. The excitation of the system to the state S_2 is visualized as an appearance of a wave packet in the vicinity of the S_2 term bottom (see Figure 2). Next are the transitions occurring at the points of terms intersection $U_{S2} = U_{CS}^{(n)}$ and populating the vibrational repetitions of the CS state (thin dashed lines in Figure 2). Upon transition the system being in nonequilibrium state participates in several relaxation processes. First, there is the intramolecular vibrational relaxation leading to vertical transitions between neighbor states, $U_{CS}^{(n)} \rightarrow U_{CS}^{(n-1)}$. Second, there is the medium relaxation that manifests itself in the motion of the wave packet to the bottom of the term $U_{CS}^{(n)}$. During this motion, the wave packet passes the term crossing points determining by the equation $U_{S1}^{(m)} = U_{CS}^{(n)}$ that results in hot transitions to the first excited state S_1. It should be noted that the intramolecular vibrational relaxation in S_1 state, $U_{S1}^{(m)} \rightarrow U_{S1}^{(m-1)}$, also plays an important role since it can pronouncedly increase the hot CR effectiveness.[7] Naturally, the final equilibrium populations of S_1 and CS states are determined by the energy gap between them. However, if the CS state is placed below the S_1 state, the hot CR can lead to considerably larger population of the S_1 state than that of equilibrium one. As a result the S_1 population is expected to rise at short time scale and to decay at longer times.

III. Results of Simulations of CS and CR Dynamics in Directly Linked Zn−Porphyrin−Imide Dyads

The CS dynamics curves for the ZP−I series are shown to be satisfactorily approximated with a single-exponential function.[12−14] Moreover, it is possible to reproduce the CS rate constants in solvents of different polarities with the well-known

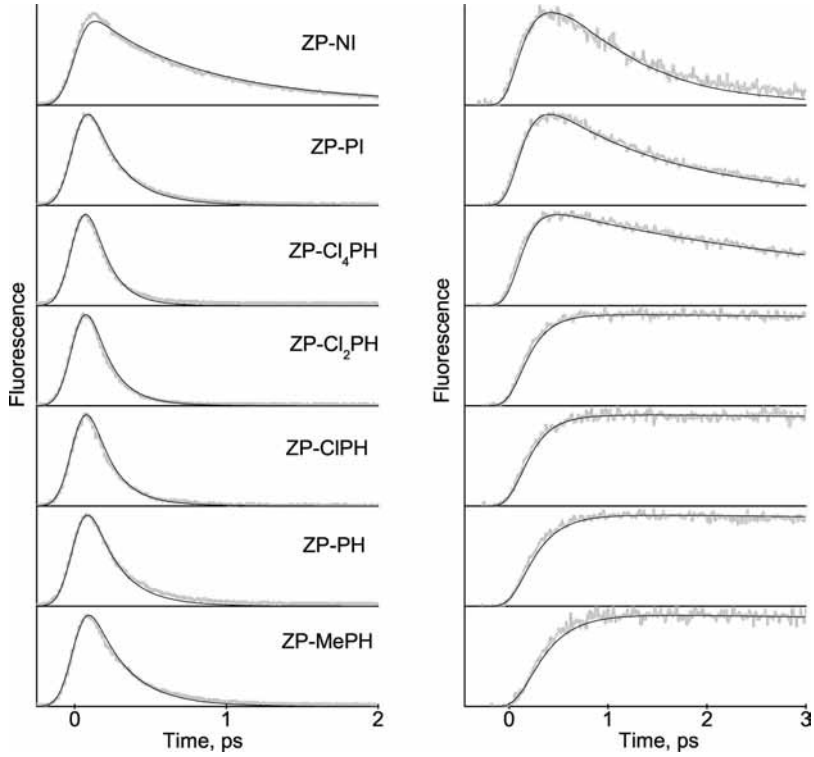

Figure 3. Population dynamics of S_2 (left panel) and S_1 (right panel) states. The data are plotted with light gray lines (experimental results)[14] and black lines (simulation results). The values of ΔG_{CS} and V_{el} are listed in Table 1. The values of other parameters being identical for CS and CR are: $E_{rm} = 0.5$ eV, $E_{rv} = 0.4$ eV, $\hbar\Omega = 0.17$ eV, $\tau_v = 0.03$ ps, $\tau_e = 0.110$ ps.

Ulstrup−Jortner equation[37,38] using the common set of energetic parameters.[13] The Ulstrup-Jortner model and the model considered in this paper describing the same process have joint parameters. Therefore the parameters obtained in ref 13 may be taken as the starting point for the simulations. Nevertheless we should emphasize that in these systems the CS timescales are shorter than the solvent relaxation times. So, the dynamic solvent effect[34,39] can not be neglected. Since the Ulstrup−Jortner model ignore totally this effect and the present model does not, a difference in the parameters is expected.

All simulations of the CS and CR dynamics are performed for tetrahydrofuran solution (THF) at room temperature, $k_BT = 0.025$ eV. The dynamic parameters of THF are used those reported in ref 40: $x_1 = 0.443$, $x_2 = 0.557$, $\tau_1 = 0.226$ ps, and $\tau_2 = 1.520$ ps. The relaxation time of the intramolecular high frequency vibrational mode is assumed to be $\tau_v = 0.030$ ps. To compare the experimental and theoretical data we have to take into account the instrumental response time. The fluorescence intensity measured in the experiments, $A(t)$, is determined as a convolution of the population of a state with the instrumental response function

$$A(t) = (\pi\tau_e^2)^{-1/2}\int_{-\infty}^{t} P(t-\tau)\exp(-\tau^2/\tau_e^2)\,d\tau \quad (3.1)$$

where $\tau_e = 110$ fs[13] is the instrumental response time.

First the CS dynamics are fitted. Using the parameters:[13] $E_{rm} = 0.5$ eV, $E_{rv} = 0.4$ eV, $\hbar\Omega = 0.17$ eV, and the CS free energy values[14] listed in Table 1, we have been able to reproduce the experimental CS rates with the electronic coupling values noticeably larger than those obtained in ref 13. This reflects a significant role of the dynamic solvent effect.

At the second stage the dynamics of both CS and CR are fitted. The same values of the medium reorganization energy for CR and CS are employed. The characteristics of intramolecular vibrational quantum mode for CR are also assumed to be equal to those of CS process. The values of CR free energy are calculated with the equation

$$\Delta G_{CR} = \Delta G_{12} - \Delta G_{CS} \quad (3.2)$$

The free energy gap between two excited states, ΔG_{12}, can be estimated from steady-state absorption spectra of ZP−I series (see Supporting Information in ref 13). The spectra show that the energies of both 0−0 transitions, $S_0 \rightarrow S_1$ and $S_0 \rightarrow S_1$, are practically the same throughout the series. So that the unique value for all molecules $\Delta G_{12} = -0.68$ eV is obtained. Then, only the electronic couplings, V_{CS} and V_{CR} are the variable parameters.

With this set of parameters a satisfactory fitting to experimental data on population dynamics of both excited states is possible. However such a fitting has at least two troubles. First, the value of V_{CR} varies nearly over an order of magnitude (0.01−0.08 eV), while the value of V_{CS} varies in the range of 0.02−0.04 eV throughout the ZP−I series. Taking into account the invariability of S_1 and S_2 absorption bands and small variation of V_{CS} in the series, it is difficult to expect such a large variation of V_{CR}. Indeed, the invariability of S_1 and S_2 absorption bands means that the porphyrin orbitals remains nearly constant. The value of V_{CS} depends on the overlap between the porphyrin orbitals and quencher orbitals and small variation of V_{CS} may be interpreted as a small variation of the quencher orbitals. In such a case a small variation of V_{CR} has to be expected. Second, for molecules with $-\Delta G_{CS} < -\Delta G_{12}$ a fast increase of the S_1 population is followed by a slower rise, whereas the experiment shows a slow decay of the S_1 population at this stage. There are at least two possibilities to avoid these troubles: either to admit a large variation of both the medium and intramolecular reorganization energies or to allow a relatively small variation of the CS free energy throughout the series. The first possibility should be excluded due to the similarity of the molecules of the series.

Thus, we assume ΔG_{CS} to be variable and we set $V_{CS} = V_{CR}$ as the first approximation to reduce the number of variable parameters. The results of simulations are presented in Figure 3 and the parameters obtained in fitting are listed in Table 1. One may see that the fitting is in a rather good agreement with experimental data and there is no necessity to vary V_{CS} and V_{CR} independently. In the dyes ZP−NI, ZP−PI, and ZP−Cl_4PH a fast rise of S_1 population is followed by rather fast decay. This decay essentially proceeds as the thermal electronic transition and its high rate is conditioned by the proximity of the transitions to the barrierless region. The S_1 populations of the dyes ZP−Cl_2PH, ZP−ClPH, ZP−PH, and ZP−MePH also decay but much slower due to a higher activation barrier between S_1 and CS states. The timescales of these decays are a few tens of ps.

Now we would like to discuss the values of ΔG_{CS} and ΔG_{CR} (see Table 1) needed for proper description of CR dynamics. For the dyes ZP−NI, ZP−PI, ZP−Cl_4PH, and ZP−Cl_2PH, the difference between ΔG_{CS} values obtained in the fitting and those found in ref 14 does not exceed 10% and is within the error of the estimation. For dyes ZP−ClPH, ZP−PH, and ZP−MePH there is a fundamental difference, namely, we obtain a positive sign of ΔG_{CR} instead of a negative one. The sign of ΔG_{CR} is a factor controlling the dynamics of S_1 population at moderate times. If a part of the dyes had negative values of ΔG_{CR}, the initial rise of the S_1 population conditioned by hot transitions during vibrational relaxation of CS state would be followed by a further rise of S_1 state population due to thermal CR. However the experimental results show rather a decay of the S_1 population in 1 - 3 ps window with the rate constants varying from 1 to 0.01 ps^{-1}. It evidences strongly in favor of ΔG_{CS} and ΔG_{CR} values obtained in the fitting.

IV. Concluding Remarks

In the present study, we have examined the mechanism of CS from the second excited state. A distinguishing feature of this process is effective hot recombination to the first excited state. This implies that CS and CR are not separable and the time scale of the S_1 state population rise is predetermined by the time scale of S_2 population decay. This regularity was deduced from the experimental data in refs 11 and 14 and is quantitatively reproduced in the framework of the model elaborated here. The dynamics of S_1 state occupation depend not only on the S_2 decay rate but on the medium and intramolecular vibration relaxation timescales too. Moreover, there is a dependence on the distribution of the sink effectivenesses at the S_2 free energy surface. The distribution, in its turn, is determined by the Franck−Condon factors and intramolecular vibration redistribution time scale. As a result, a quantitative description of dynamics of the CR into the first excited-state requires a solution of full dynamical many-level problem.

Despite the fact that a good fitting to experimental data has been obtained, there are some weaknesses in the model. One of them is the intramolecular reorganization description in terms of single vibrational high-frequency mode. In actuality in an electronic transition there are several active vibrational modes. For example, the resonance Raman spectra of donor−acceptor complexes show that about ten vibrational modes associate with charge transfer transition.[20,41,42] In this case the role of the reorganization of the intramolecular high-frequency vibrational modes in hot CR pronouncedly increases. This is conditioned by a huge number of relatively weak sinks on the CS state free energy surface. Despite the sinks weakness, the total probability of hot CR approaches unity due to their vast number.[20] If real frequencies and the Franck−Condon factors of vibrational modes are used instead of the characteristics of the single effective mode, the time scale of CR would change insignificantly but maximum S_1 population could rise considerably. To put it differently, the fitting to normalized S_1 population is expected to be weakly sensitive to the number of active vibrational modes that justifies the application of the simplified single mode model in this case. However, if the absolute values of S_1 population were known, the real frequencies and the Franck−Condon factors of vibrational modes would be required for proper fitting.

Acknowledgment. We are indebted to Dr S. Feskov for his help in writing the simulation code. This work was supported by the Russian foundation for basic research (Grant No. 08-03-00534).

References and Notes

(1) Najbar, J.; Dorfman, R. C.; Fayer, M. D. *J. Chem. Phys.* **1991**, *94*, 1081.
(2) Gladkikh, V.; Burshtein, A. I.; Feskov, S. V.; Ivanov, A. I.; Vauthey, E. *J. Chem. Phys.* **2005**, *123*, 244510.
(3) Tachiya, M.; Murata, S. *J. Am. Chem. Soc.* **1994**, *116*, 2434.
(4) Walker, G. C.; Akesson, E.; Johnson, A. E.; Levinger, N. E.; Barbara, P. F. *J. Phys. Chem.* **1992**, *96*, 3728.
(5) Bagchi, B.; Gayathri, N. *Adv. Chem. Phys.* **1999**, *107*, 1.
(6) Feskov, S. V.; Ionkin, V. N.; Ivanov, A. I. *J. Phys. Chem. A* **2006**, *110*, 11919.
(7) Mikhailova, V. A.; Ivanov, A. I. *J. Phys. Chem. C* **2007**, *111*, 4445.
(8) Ivanov, A. I.; Potovoi, V. V. *Chem. Phys.* **1999**, *247*, 245.
(9) Pagès, S.; Lang, B.; Vauthey, E. *J. Phys. Chem. A* **2004**, *108*, 549.
(10) Asahi, T.; Mataga, N. *J. Phys. Chem.* **1989**, *93*, 6575.
(11) Mataga, N.; Shibata, Y.; Chosrowjan, H.; Yoshida, N.; Osuka, A. *J. Phys. Chem. B* **2000**, *104*, 4001.
(12) Mataga, N.; Chosrowjan, H.; Shibata, Y.; Yoshida, N.; Osuka, A.; Kikuzawa, T.; Okada, T. *J. Am. Chem. Soc.* **2001**, *123*, 12422.
(13) Mataga, N.; Chosrowjan, H.; Taniguchi, S.; Shibata, Y.; Yoshida, N.; Osuka, A.; Kikuzawa, T.; Okada, T. *J. Phys. Chem. A* **2002**, *106*, 12191.
(14) Mataga, N.; Taniguchi, S.; Chosrowjan, H.; Osuka, A.; Yoshida, N. *Chem. Phys.* **2003**, *295*, 215.
(15) Morandeira, A.; Engeli, L.; Vauthey, E. *J. Phys. Chem. A* **2002**, *106*, 4833.
(16) Rosenthal, S. J.; Xie, X.; Du, M.; Fleming, G. R. *J. Chem. Phys.* **1991**, *95*, 4715.
(17) Maroncelli, M.; Kumar, V. P.; Papazyan, A. *J. Phys. Chem.* **1993**, *97*, 13.
(18) Jimenez, R.; Fleming, G. R.; Kumar, P. V.; Maroncelli, M. *Nature* **1994**, *369*, 471.
(19) Gumy, J. C.; Nicolet, O.; Vauthey, E. *J. Phys. Chem. A* **1999**, *103*, 10737.
(20) Feskov, S. V.; Ionkin, V. N.; Ivanov, A. I.; Hagemann, H.; Vauthey, E. *J. Phys. Chem. A* **2008**, *112*, 594.
(21) Bakhshiev, N. G. *Opt. Spectrosc. (USSR)* **1964**, *16*, 446.
(22) Hizhnyakov, V.; Tekhver, I. Yu. *Phys. Status Solidi* **1967**, *21*, 75.
(23) Mazurenko, Yu. T.; Bakhshiev, N. G. *Opt. Spectrosc. (USSR)* **1970**, *28*, 490.
(24) Zusman, L. D.; Helman, A. B. *Opt. Spectrosc. (USSR)* **1982**, *53*, 248.
(25) Bagchi, B.; Oxtoby, D. W.; Fleming, G. R. *Chem. Phys.* **1984**, *86*, 25.
(26) Van der Zwan, G.; Hynes, J. T. *J. Phys. Chem.* **1985**, *89*, 4181.
(27) Loring, R. F.; Yan, Y. J.; Mukamel, S. *J. Chem. Phys.* **1987**, *87*, 5840.
(28) Coalson, R. D.; Evans, D. G.; Nitzan, A. *J. Chem. Phys.* **1994**, *101*, 436.
(29) Cho, M.; Silbey, R. J. *J. Chem. Phys.* **1995**, *103*, 595.
(30) Domcke, W.; Stock, G. *Adv. Chem. Phys.* **1997**, *100*, 1.
(31) Jean, J. M. *J. Phys. Chem. A* **1998**, *102*, 7549.
(32) Barzykin, A. V.; Frantsuzov, P. A.; Seki, K.; Tachiya, M. *Adv. Chem. Phys.* **2002**, *123*, 511.
(33) Ivanov, A. I.; Belikeev, F. N.; Fedunov, R. G.; Vauthey, E. *Chem. Phys. Lett.* **2003**, *372*, 73.
(34) Zusman, L. D. *Chem. Phys.* **1980**, *49*, 295.
(35) Ivanov, A. I.; Ionkin, V. N.; Feskov, S. V. *Russ. J. Phys. Chem. A* **2008**, *82*, 303.
(36) Fedunov, R. G.; Feskov, S. V.; Ivanov, A. I.; Nicolet, O.; Pagès, S.; Vauthey, E. *J. Chem. Phys.* **2004**, *121*, 3643.
(37) Ulstrup, J.; Jortner, J. *J. Chem. Phys.* **1975**, *63*, 4358.
(38) Jortner, J. *J. Chem. Phys.* **1976**, *64*, 4860.
(39) Burshtein, A. I.; Yakobson, B. I. *Chem. Phys.* **1980**, *49*, 385.
(40) Horng, M. L.; Gardecki, J. A.; Papazyan, A.; Maroncelli, M. *J. Phys. Chem.* **1995**, *99*, 17311.
(41) Markel, F.; Ferris, N. S.; Gould, I. R.; Myers, A. B. *J. Am. Chem. Soc.* **1992**, *114*, 6208.
(42) Kulinowski, K.; Gould, I. R.; Myers, A. B. *J. Phys. Chem.* **1995**, *99*, 9017.

JP806589M